A Characterization of Tropical Transient Activity in the CAM3 Atmospheric Hydrologic Cycle

Philip J. Rasch[1], Mark J. Stevens[1], Lucrezia Ricciardulli[2], Aiguo Dai[1],
Andrew Negri[3], Robert Wood[4], Byron A. Boville[1], Brian Eaton[1], James J. Hack[1]
National Center for Atmospheric Research[5]

Printed: January 2, 2005

For J. Climate CCSM Special Issue

Corresponding Author: P. Rasch: (303)-497-1368 (office), pjr@ncar.ucar.edu

[1]NCAR, P.O. Box 3000-80307, Boulder CO 80307
[2]Remote Sensing Systems, 438 First Street, Suite 200, Santa Rosa, CA 95401 USA
[3]NASA/GSFC, Laboratory for Atmospheres, Code 912, Greenbelt, MD, 20771
[4]Dept. of Atmospheric Sciences, Box 351640, University of Washington, Seattle, WA 98195
[5]The National Center for Atmospheric Research is sponsored by the National Science Foundation

Abstract

The CAM3 is the latest generation of a long lineage of general circulation models produced by a collaboration between NCAR and the scientific research community. Many aspects of the hydrological cycle have been changed relative to earlier versions of the model. It is the goal of this paper to document some aspects of tropical variability of clouds and the hydrologic cycle in CAM3 on time scales shorter than 30 days and to discuss the differences compared to the atmosphere and earlier model versions. We focus on cloud top brightness temperature, precipitation, and cloud liquid water path. We have explored the transient behavior of the model to changes in resolution, numerical method used to solve the equations for atmospheric dynamics and transport, and to the underlying lower boundary condition of sea surface temperature and surface fluxes. We have pointed out that interannual variability of tropical features make it difficult to produce a clear picture of short time scale behavior in the model and atmosphere.

We have shown that the ratio of stratiform to convective rainfall is much too low in CAM3, compared to observational estimates. It is much higher in CAM3 (10%) than the CCM3 (order 1-2%), but is still a factor of 4-5 too low compared to observational estimates. We show that some aspects of the model transients are sensitive to resolution. Higher resolution versions of CAM3 show too much variability (both in amplitude and spatial extent) in brightness temperature on time scales of 2-10 days compared to observational estimates. Precipitation variance is underestimated on time scales from a few hours to 10 days compared to observations over ocean, although, again the biases are reduced compared to previous generations of the model. The diurnal cycle over tropical land masses is somewhat too large, and there is not enough precipitation during evening hours. The model tends to produce maxima in precipitation and liquid water path that are a few hours earlier than that seen in the observations over both oceans and land.

1 Introduction:

Transient activity in cloud processes and precipitation are an important component of the atmosphere and the Earth's climate. Indeed, clouds are by their very nature transient. Yet, it is a frequent experience with general circulation models (GCMs) that clouds' transient aspects are quite different from that seen in the atmosphere (Ricciardulli and Garcia, 2000; Dai and Trenberth, 2004; Scinocca and McFarlane, 2004; Yang and Slingo, 2001), even when the spatial patterns are reasonable.

When viewed from the larger scale ($>$ 100 km), there are both a pseudo-random component to clouds, as well as a component that is strongly correlated with other meteorologically important features. Clouds show variations on time scales varying from seconds to decadal lengths. This paper focusses on aspects of clouds associated with time scales shorter than monthly lengths. Longer time scale features are discussed in Boville et al. (2004) and Hack et al. (2004).

The shorter time scale properties of clouds are important to the climate system for a variety of reasons. On the shortest of the time scales resolvable by large scale models (order an hour to a day), clouds are involved in rapid transports of heat, moisture, momentum, and atmospheric trace constituents. In the tropics, where nearly all of the solar variance is diurnal (as opposed to seasonal), clouds act as the strongest modulators of the variability associated with solar forcing (Bergman and Salby, 1996). The vigorous motions associated with latent heat release can introduce oscillations in the atmosphere that propagate to and influence regions far from their source (Ricciardulli and Garcia, 2000). The breakdown of gravity waves excited by convection can drive major modes of the middle atmosphere like the semi-annual and quasi-biennial oscillation (QBO, e.g., Takahashi (1999)). On longer time scales clouds features participate strongly in regulating and interacting with other dynamical features like squall lines, Madden-Julian oscillations (MJO, mid-latitude frontal storms and a host of other atmospheric phenomena.

In regions of the atmosphere where latent heat release drives atmospheric dynamics less strongly, clouds play other roles. Their modulation of solar insolation, and the radiative cooling near cloud top act to strongly influence the atmospheric boundary layer. The transports of heat and moisture throughout the boundary layer are thus strongly modulated by clouds, and this in turn plays a role in the venting of other important trace constituents like water, through short lived species, (CH3I, radon to long lived species like CO2). The role of the boundary layer and convective processes in rectification of trace species (e.g. Denning et al. (1996)), and transport are discussed in more detail in Rasch (2004) elsewhere in this issue.

Many of the diagnostics similar to those employed in this paper have been used before to analyze earlier versions of the NCAR general circulation models (GCMs) and climate models. Ricciardulli and Garcia (2000) described the response of equatorial waves to deep convective forcing in the Community Climate Model (CCM3). Collier and Bowman (2004) described the behavior of the diurnal variation of tropical precipitation in CCM3, using prescribed ocean surface temperatures. Ricciardulli and Sardeshmukh (2002) documented the local time and space scales of organized convection using satellite retrievals of a proxy for convection and compared those results to CCM3 and another model. Dai and Trenberth (2004) documented the behavior of the diurnal variation of precipitation, clouds, and other fields in the Community Climate System Model version two (CCSM2), a coupled model which utilized the CAM2 (CAM version 2) for its atmospheric component. The atmospheric GCM communicated with the ocean model component of the coupled system once per day. This restricted the ability of the ocean surface to respond to changes in the forcing, and thus affects the diurnal variation of convection and precipitation. Dai and Trenberth (2004) attributed part of the weak diurnal variation in the CAM2 over oceans to this lack of a diurnal variation in surface temperature and fluxes.

Although many of the papers cited in the previous paragraph are quite recent, CCM3 was released in 1996, CAM2 was released in 2001, and a variety of important

changes have occurred in our model framework in the 9 years since then. These changes have the potential to change the variability of the cloud processes in the model, and the response of the model to changes in variability. In addition to changes in model physics and dynamics, the model can be run in a much broader variety of configurations than previous versions of our GCM. This allows us to examine the sensitivity of the transient aspects of clouds to resolution, lower boundary conditions, and formulation for large scale dynamics. It is the goal of this paper to document some aspects of the simulation of cloud variability in CAM3 to these variations, and contrast CAM3's behavior with the behavior of previous generations of the model.

2 Description of CAM3 Configurations

Since a description of components of CAM3 can be found in other papers appearing in this special issue, we point the reader to the relevant papers describing the components, and highlight changes to our GCM from the CCM3 version that can influence the model variability.

A general overview of the CAM3 is provided in Collins et al. (2004a). The formulation for the hydrologic cycle can be found in Boville et al. (2004). The climatological (seasonal and longer) time scale features of the hydrologic cycle simulation can be found in Hack et al. (2004). The sensitivity of the model to horizontal resolution is discussed in Hack (2004). The use of the slab ocean, which allows the sea surface to respond to changes in fluxes at the ocean surface is discussed in Kiehl et al. (2004). Full details of all aspects of the formulation can be found in the NCAR technical note (Collins et al., 2004b).

It is worthwhile to discuss some changes that could influence the model cloud variability, and highlight some areas which remain unchanged that also may affect it. CCM3 used a prescribed cloud water formulation. The cloud condensate distribution was specified to be a simple function of the vertical integral of water vapor.

The latent heat of fusion associated with phase change between ice and liquid was ignored. CAM2 and CAM3 employ a prognostic cloud condensate parameterization. The CAM2 employed a simpler condensate variable that distinguished less strongly between water and ice, and rain and snow. CAM2 also neglected latent heat of fusion, advection and sedimentation of condensate, and some evaporation terms. CAM3 condensed water substances represented in the model include:

- small liquid and ice particles that evolve dynamically in response to advection, conversion to precipitating forms, phase changes (between liquid, ice and vapor), sedimentation, and turbulent transport;

- large liquid and ice particles (rain and snow/graupel) that are assumed to be in steady state with their sources.

In CCM3, convection could only detrain water vapor, and cloud water was insensitive to local detrainment. In CAM3 the convection is allowed to detrain condensate and water vapor, and these fields feed the stratiform clouds. In CCM3 precipitation fell to the surface. In CAM3, precipitation can evaporate as it falls. These features, and changes to radiation, cloud overlap, the land model, and other things, have produced substantial changes to the water vapor, liquid and ice distributions and the associated radiative and thermodynamic balances, and many facets of the model climate between CAM3 and CCM3. Of course with reformulations of this extent changes to tunable parameters were also required.

We have examined the transient behavior in 6 different model configurations described in table 1. These configurations explore the model sensitivity to resolution, to the method used to calculate the sea surface temperature, and to the numerical method used to solve the atmospheric dynamics. Because the solution is sensitive to resolution, and numerics, when these model aspects are changed, small changes in a few tunable parameters are required to produce similar climates in the time mean. We have not examined the transient sensitivity of the model to changes in these pa-

rameters, although the transient behavior of model may be sensitive to changes to them. Scinocca and McFarlane (2004) have shown that the transient behavior of the Zhang-McFarlane scheme used for deep convection in CAM3 is quite sensitive to the setting of certain constants within that parameterization. Such an exploration is certainly merited, but initially we have decided to document our current formulations. We intend future studies to explore the sensitivity of our model to parameterization settings, and the parameterizations themselves. Dai and Trenberth (2004) speculated that the global diurnal cycle deficiencies in CCSM2 over ocean were associated in part to the lack of a diurnal cycle in CAM. In most configurations of CAM3 and CCSM the sea surface temperature (SST) is held fixed over each 24 hour time period. The standard atmosphere only versions of CAM3 fix the SST, and update it once per day to a value interpolated from data read in from an external dataset. In the standard version of the coupled model (CCSM3), CAM3 communicates with the ocean model once per day, and the SSTs are again held fixed for a 24 hour period. In the slab ocean model (SOM) configurations the SSTs are allowed to evolve in time and to respond to changes in the net radiation, and surface fluxes associated with changing wind speed. Therefore the SOM model configuration provides an opportunity to explore the sensitivity of the model transient activity to a varying SST.

All model versions were started at near equilibrium conditions and run for 5 years. The versions of the model identified as having a 128x64 resolution horizontal cell dimensions of approximately 2.8 degrees on a side. The FV model employs a 2x2.5 degree regular latitude/longitude grid with cell centers located at poles and equator. There are approximately 60% more points on the globe than the 128x64 grid model configurations. The T85 model is precisely twice as many points in latitude and longitude as the 128x64 for a factor of four increase in resolution.

Case	Resolution	dynamics	SST	timestep (s)
T42amip	128x64	Spectral/FD	prescribed 1950-1954	1200
T42som	128x64	Spectral/FD	predicted SST	1200
SLDamip	128x64	Semi-lagrangian/FD	prescribed 1950-1954	3600
FVamip	144x91	Control volume	predicted SST	1800
FVsom	144x91	Control volume	prescribed 1950-1954	1800
T85amip	256x128	Spectral/FD	prescribed 1950-1954	600

Table 1: The cases examined in this study, ordered from lowest to highest resolution. Note that although the semi-lagrangian and spectral T42 models contain the same number of gridpoints the former model does not use the inherent smoothing required for a spectral transform model. FD stands for Finite Difference.

3 Convective versus Stratiform precipitation

Many interesting cloud features that are associated with convection occur on short time scales, and it is important to identify the partitioning between cloud phenomena undergoing vigorous convection and that associated with the less vigorous motions associated with decaying convective elements and frontal motions. In the tropics, where more than half the global precipitation occurs, the partitioning is believed to be shared approximately equally between convective and stratiform precipitation (Schumacher and Houze, 2003; Houze, 1997). The vertical distributions of heating associated with precipitation occur with very different distributions for convective and stratiform processes (Houze et al., 1980). Convective heating is generally believed to be positive throughout the vertical profile, with the height of the maximum depending on the size spectrum of the convective elements, while the heating maximum occurs the mid- and upper troposphere for stratiform process, with cooling below. Also, the areal extent of the clouds associated with vigorous updrafts are believed to be only a few percent with a much larger radiative contribution from stratiform clouds (LeMone and Zipser, 1980; Jorgensen and LeMone, 1989). Hartmann et al. (1984)

showed that a reasonable large scale tropical dynamical response to the heat release by tropical precipitation required both convective and stratiform components.

A useful, quantitative global picture of the partitioning between convective and stratiform rainfall estimates can be achieved by comparing the Tropical Measuring Mission (TRMM) Precipitation Radar (PR) to the CAM3 precipitation. Although the PR and TRMM Microwave Imager (TMI) datasets provide some of the best global characterizations of precipitation available today (Kummerow et al., 2000) they are not without deficiencies. TRMM was launched in a precessing orbit that allows relatively complete coverage of the earth between 38N and 38S, observing a given location about once per day, at a different time each day, with a cycle of about 46 days. Since precipitation is highly variable in space and time, the sampling error is significant. Negri et al. (2002a) have estimated the biases in hourly rain rates for 5x5 degree grid estimates to be 15-48% for PR and 13-34% for TMI. Negri et al. (2002b) found a bias in TMI of 33% compared to monthly mean regional estimates from raingauges for the same period. Bowman et al. (2003) found much very small biases for TMI and about 30% biases for PR compared to tropical pacific buoy raingauge data. Kummerow et al. (2000) showed 24% differences between TMI and PR retrieval of monthly mean estimates of global tropical precipitation. Masunaga et al. (2002) explained these differences in terms of biases in the assumed vertical profiles of cloud water content, and ambiguities in the attenuation correction in heavy precipitation around tropical rainfall maxima. These uncertainties result in biases. TMI underestimates near surface condensed water in midlatitude winter and PR underestimates of the vertically integrated water path in the tropics. The consequence is that PR rainrate estimates tend to be much lower than TMI rainrate estimates in the tropics, and the two are much closer to each other at midlatitudes.

Figure 1 shows the annual averaged rainfall estimates for TRMM PR (TRMM dataset 3A25, composited from 1998-2003 at about 0.5 degree resolution) and a 5 year average of the T85 version of CAM. CAM and TRMM total precipitation esti-

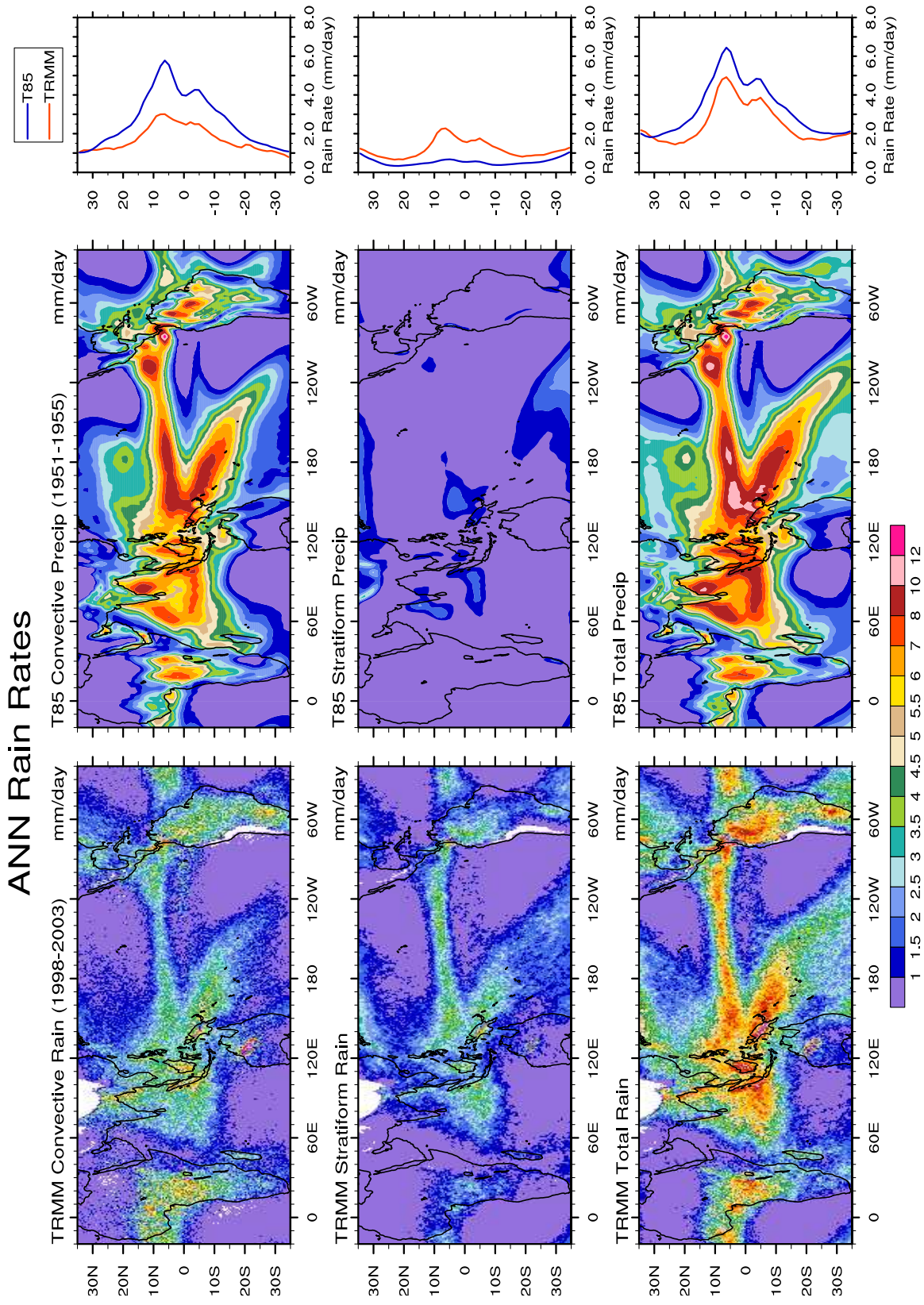

Figure 1: Annual average of convective and stratiform precipitation estimates from TRMM at T85 resolution and CAM3 at T85 resolution.

mates (lower panels) agree qualitatively, CAM3 is higher globally than the TRMM estimate. As discussed previously, The TRMM PR retrievals are always lower the TMI in the tropics, and the TMI product agrees much more closely with the CAM global total (stratiform plus convective) precipitation (not shown). Although the total precipitation is in reasonable agreement with CAM, the partitioning between stratiform and convective rain is very different. This signal is similar to that seen with CCM3 in Song and Yu (2004). They reported stratiform rain accounting for 1.5% of the total rainfall between 20N and 20S. This simulation shows stratiform precipitation to be about 10% of the total rain, which is closer to, but still much lower than the TRMM estimates. The amount of stratiform rainfall in the model is sensitive to resolution. The T31 and T42 simulations show much less stratiform rain in the tropics (not shown). Dai and Trenberth (2004) suggested that the underestimate of stratiform precipitation in CCSM2 was related to deficiencies in the moist convection scheme. They hypothesized that moist convection occured too frequently, and lasted too long, removing water vapor prematurely and too efficiently. We show that this hypothesis is consistent with CAM3 behavior as well in section 6.

4 Issues of Interannual variability

Any analysis of short time scale clouds features is complicated by issues of interannual variability. In our case the differences in variability associated with regime change, and the simultaneous existence of clouds with differing characteristics are the issue. As an example, figure 2 shows the behavior of a number of fields at a single grid-point in space for two consecutive seasons of the months of December, January, and February (DJF) in a T42 configuration of the model. This model uses sea surface temperatures (SSTs) from a climatology constructed by taking the ensemble average of approximately 20 years worth of monthly mean observed SST data. Therefor the SST repeat annually and interannual variability from external forcing (eg ENSO) can

not explain the variation in the simulation.

The point of focus is located near 45°E, 1°S, in the south Indian Ocean, just off the African Coast . The upper panels of the figure show time series (at 3 hour intervals) of vertically integrated liquid water path, low cloud fraction, convective precipitation and stratiform precipitation for that model grid point. The liquid water path represents the average value within the column including cloudy and cloud free areas. The lower panels show diurnal cycle composites derived by determining the local hour of the day for each time sample, and averaging all time samples with that particular local hour value. In the lower panels, we have partitioned the diurnal cycle composites three ways: an average diurnal cycle for DJF(year 1) (thin solid line); an average value for DJF(year 2) (dashed line); and the average value for years 1 and 2 combined (thick solid line). A number of interesting features are evident in the figure.

- The behavior of DJF(year1) is different from that of DJF(year2). Ratios of the mean value during DJF(year1) and the mean value during DJF(year2) vary substantially for each field, DJF(year 1) being characteristically 2-4 time higher than DJF(year 2), and the phase of the diurnal variation is also quite different.

- Stratiform rain in CAM3 is not always small in the tropics, as can be seen in the upper panels. The maximum in instantaneous stratiform rain is actually higher than the convective rain at some times during DJF(year1).

- The diurnal cycle inferred separately from the two years differ from each other. Year 1 was characterized by high liquid water path (LWP), and stratiform drizzle in the afternoon, at about 15-17 Local Solar Time (LST), high convective precipitation and cloud cover occur in the early morning. Year 2 shows maximum LWP, cloud cover and stratiform precipitation in the early morning hours (4-6LST), and highest convective precipitation in the early afternoon.

- The composite of the two seasons combined is a confusing meld of the two individual years. The diurnal cycle of the LWP, and stratiform and convective

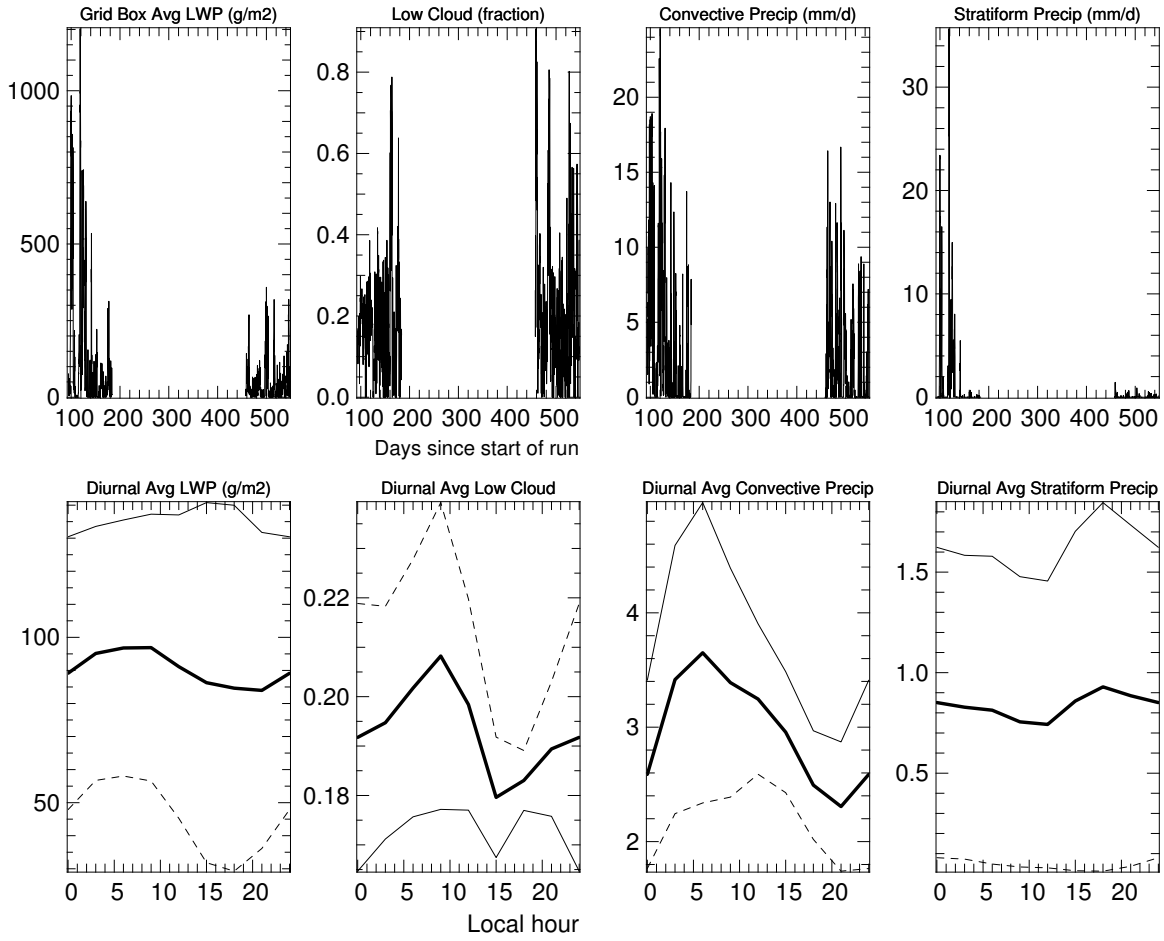

Figure 2: Upper panels show the time series of various fields for two adjacent December, January, February (DJF) seasons at one model gridpoint. The time is in days with origin at the begining of the model run. Lower panels show the composite diurnal average for each of seasons. The thin solid line is the average for the first season. The dashed line is the second season. The thick solid line represents the average of the two seasons.

precipitation reflect the character of year 1, while the cloud cover variations reflect the character of year 2.

- While we have not performed a formal error characterization of in this figure, one could utilize the "year1" and "year2" estimates to be a crude estimate of the error in the mean of the two years, in which case the error bars would span the range defined by the year1 and year2 estimates. would imply that

The distinctly different diurnal behavior between year 1 and year 2 suggests shifts in climatological features at that location. During year 1 the models behavior is reminiscent of an area of strong convective activity with precipitation peaking in early morning hours and cloud optical depth/thickness peaking in early afternoon. During year 2, the model grid point looks more like a stratocumulus region, with lower precipitation rates, and a peak in cloud optical thickness in the early morning hours. The existence of more than one type of cloud behavior occurring has previously been recognized as important in characterization of tropical ocean convection (Meisner and Arkin, 1987; Janowiak et al., 1994; Yang and Slingo, 2001).

This suggests that a desirable strategy in characterizing atmospheric transients is to stratify the data in some manner prior to the data reduction, analysis, or compositing, to isolate out particular phenomena of interest. Hendon and Woodberry (1993) utilized a Deep Convective Activity (DCA) index defined as to be nonzero only where cold, optically thick clouds were present in a scene, to identify times and locations of vigorous convection. Ricciardulli and Sardeshmukh (2002) use only months in which DCA was non-zero at least 5% of the time in their analysis of convection using the GCI dataset described below, in order to focus their attention only on rain events rather than seasonal variation of the spatial patters on rain. We have explored a variety of mechanisms in our attempts to stratify the data. When these strategies result in a clarification of the interpretation we discuss them. Otherwise we show analyses based on 5 year averages/composites of the data in the rest of this paper.

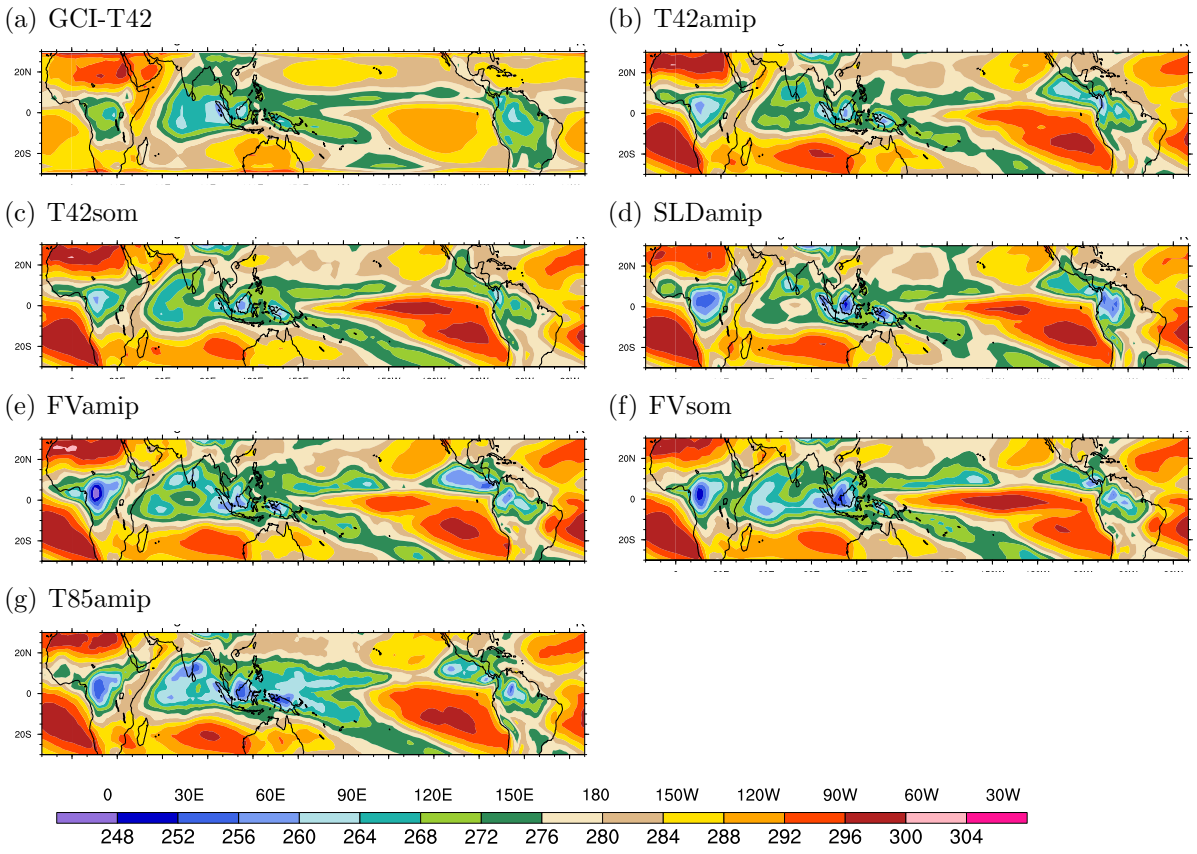

Figure 3: Annual average T_{11}^B from the GCI dataset of Salby et al. (1991) and CAM3 simulations.

5 Brightness Temperature Analysis

There are obvious difficulties in global characterizations of the higher frequency components of clouds, precipitation and convection using either rain gauge, or instruments with a narrow field of view on a precessing orbit, or sun synchronous satellites. One of the most frequently used, and useful quantities for characterization of clouds is the 11μm brightness temperature (hereafter T_{11}^B). The brightness temperature in the infrared window region (10.2-12.2 μm) provides a well understood measure of the temperature at the top of optically thick clouds. The brightness temperature has been used as a way to characterize diurnal variability of clouds (Salby et al., 1991; Bergman and Salby, 1996; Yang and Slingo, 2001), deep convective activity (Hendon and Woodberry, 1993; Bergman and Salby, 1994), precipitation Richards and Arkin (1981); Adler and Negri (1988); Arkin and Meisner (1987); Huffman et al. (1997), and many other cloud aspects.

Here, we use the Global Cloud imagery (GCI) observational estimates of T_{11}^B from Salby et al. (1991). The version of the dataset we used is discussed in Ricciardulli and Garcia (2000). This dataset includes inter-calibrated measurements from four geostationary and two polar orbiting satellites. The dataset contains synoptic estimates of global cloud fields at three hour intervals between 1983 and 1992 at about a half degree resolution. There are occasional missing data periods in this dataset. When there are occasional missing single time samples, they are replaced with the interpolated values from the time sample on either side of the missing sample. To avoid problems with interpretations of this field at the substantially different resolutions of the model and the GCI dataset we produce an area-weighted mean T_{11}^B at two model resolutions, T85 (approximately 1.4° in latitude and longitude), and T42 (approximately 2.8° in latitude and longitude). Like Yang and Slingo (2001), we focus on both precipitation, and T_{11}^B as useful quantities in interpreting transients features of the tropical atmosphere.

Minnis et al. (1991) showed that extremely high correlations exist between narrow band and broadband total longwave fluxes, and showed that a quadratic relationship could be used to estimate the value of one from the other to an accuracy of a few percent in derived flux. We use this relationship to produce an estimate of the narrow band flux from the model top of atmosphere net longwave flux, The conversion from broadband to narrowband radiances is done using relationships given in Minnis et al. (1991). They correlated infrared window (10.2–12.2 μm) data from the Geostationary Operational Environmental Satellite (GOES) with longwave (5.0–50.0 μm) data from the Earth Radiation Budget Experiment (ERBE). The best global fit for data over ocean was given by $M_b = 90.54 + 3.568M_n$ and over land by $M_b = 77.64 + 4.397M_n - 0.0111M_n^2$ where M_b and M_n are respectively broadband and narrowband estimates in Wm^{-2}. First the broadband flux as predicted by the model is converted to a narrowband radiance in the 10.2–12.2 μm window used by satellites. Then the narrowband radiance is converted to an equivalent black body temperature. A procedure that is similar in spirit was used in Yang and Slingo (2001) following Ohring et al. (1984).

Because there are occasionally missing months in the dataset and we are restricting our analysis to shorter time scales it is convenient to analyze each month individually, thus producing information on time scales from 6 hours to $\sim$30 days. Within each monthly dataset we calculate the time mean, the variance over all resolved frequencies, the partitioned variance (into three bins: $<$ 2 day periods, 2-10 day periods, and $>$ 10 day periods) and the time of maximum T_{11}^B. We estimate the local time of the maxima in brightness temperature by the compositing technique described in section 4, then fit a sinusoid to the first diurnal harmonic of the composite for phase and amplitude.

Given a characterization of the mean, variance, and hour of brightness temperature maximum, we then composite all realizations of a particular month (eg all Januarys) to form a "climatological" January. (The hour of local maximum is calculated by

converting the phase shift back to coefficients of the sinusoids, averaging ensemble members,, and then converting back to the phase shift). This produces 12 monthly samples, which we can use to produce annual and seasonal averages characterizing these fields, using similar averaging procedures.

A comparison of T_{BR} is shown in figure 3. As expected, all the models configurations agree reasonably well with the basic features of the observations, because the field is explicitly a function of the outgoing longwave radiation (OLR), and a reasonable reproduction of the time mean OLR is one of the features the model is required to reproduce. The features are consistent with longwave cloud forcing and OLR biases described in other papers in this issues. The role of clouds in the subtropical subsidence regions are underestimated, with too low cloud forcing and too high OLR, resulting in T_{11}^B that is too high in these regions. The role of clouds in the ITCZ regions is overestimated with too high cloud forcing and too low OLR, with too low T_{11}^B there.

The annually averaged estimate of total variance of T_{11}^B is shown in figure 4. The model variance increases monotonically as the resolution increases across the spectrum of model configurations. This is true regardless of whether one examines the same dynamical core (panels b and g) or between dynamical cores (panels b, d, and e). Note that the SLD dynamics resolve slightly smaller spatial scales than the spectral T42 models on the equivalent grid because there is no "spectral truncation" of most of the state variables. The finite volume configuration has a higher resolution than either the T42 or SLD model configurations. Panels (a) and (h) show the observed brightness temperatures estimates calculated at the lowest model resolution (T42, top) and at the highest model resolution (T85, bottom). It is clear that the variance calculation is sensitive to resolution, as it should be, because more features are resolved as the resolution increases, but it is also apparent that the models tend to overpredict the variance compared to the GCI data at the same resolution.

The figure indicates that substantial differences between model configurations

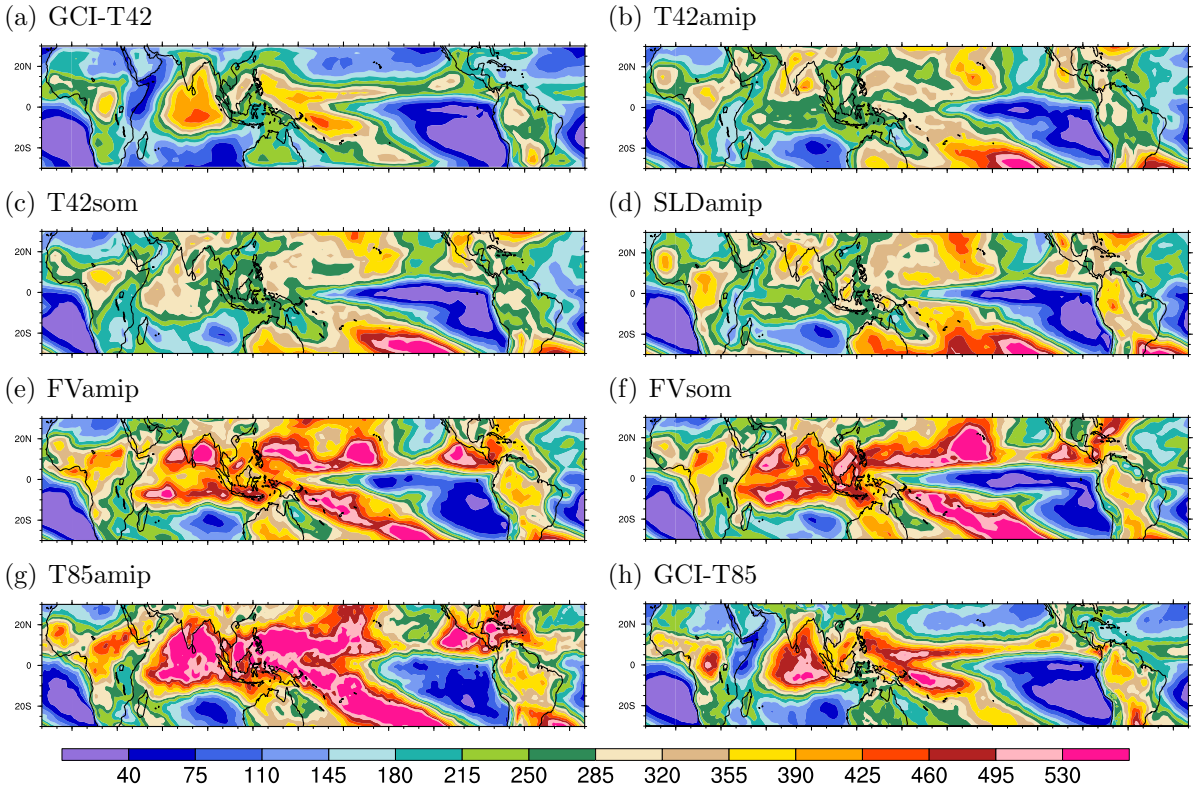

Figure 4: Annual average of the variance of T_{11}^B from the GCI dataset of Salby et al. (1991) and the CAM3 simulations. Units (K^2)

exist despite efforts to produce model configurations tuned carefully to provide a close agreement with observations in terms of seasonal and annual averages. The lower resolution model tends to miss much of the variance seen in the areas of deepest coldest convection (the warm pool, equatorial Indian ocean, and south pacific convergence zone). This is not the case for the higher resolution configurations where the models do capture these features, and indeed overestimate the variance. Near the equator, maxima in variance tend to track the minimum in time mean variance following the ITCZ. Models show areas of excessive variance in mid pacific at 30N and 30S not see in observational estimates.

One can avoid a focus on the biases associated with spatial patterns of the variance by examining the joint distribution functions of the mean value and variance of T_{11}^B. These distributions for model and GCI retrievals are shown in figure 5. The figure suggests that that both observations and models have a bimodal distribution, with a very strong peak at warm brightness temperatures corresponding to a T_{11}^B variation near the surface, and a weaker secondary peak corresponding to clouds with a top at much higher altitudes. The higher resolution model configurations show a non-zero variance over a broader range of temperatures than the GCI estimates. The observations have a more narrowly peaked spectrum than the model. There is no evidence for substantial difference in variance between models with interactive ocean surface temperatures (SOM) compared to fixed SSTs (see panels (b) and (c), or (e) and (f) for the T42 or FV model configuration respectively).

Panels (a) and (h) indicate variance is resolution dependent, since the underlying data for these figures were produced from the same high resolution dataset, but more variance is found in the upper left quadrant of the high resolution data (h)than the lower resolution version (a). The same phenomena is found in the model. The lower resolution model (panel b) has a local maximum below the 20 K reference line while the local maximum is above that line for the equivalent high resolution model configuration (g).

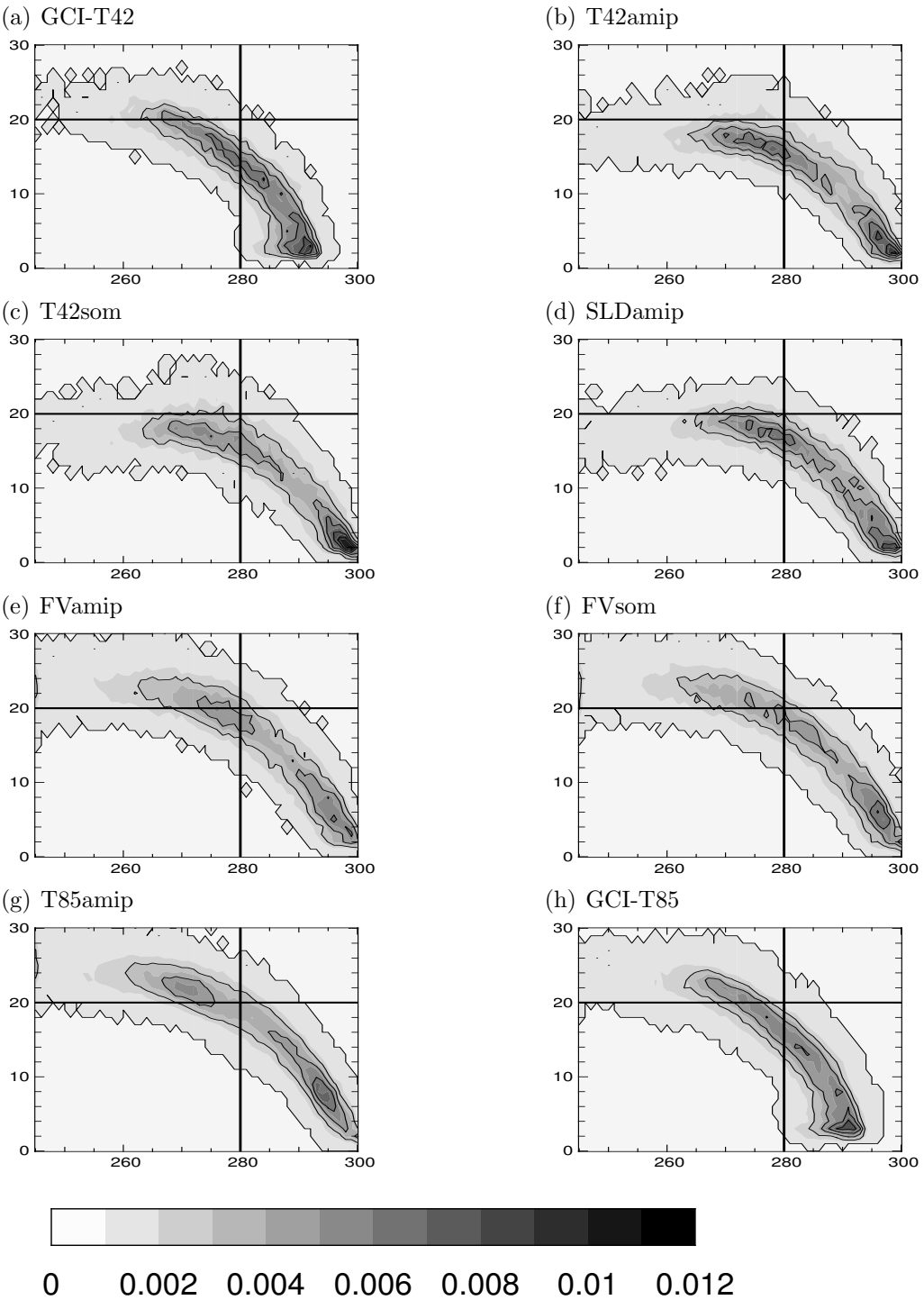

Figure 5: Joint distribution (frequency of occurrence) plotted over oceans only between 20N and 20S as a function of the standard deviation of T_{11}^B (ordinate) and monthly mean of T_{11}^B (abscissa). Normalized so the integral over the area of the figure is 1. Reference axis are displayed on the figure to highlight the evolution of the local maximum associated with high cold clouds with large variance.

The total variance has been partitioned in figure 6 into contributions on different times scales in a manner similar to Ricciardulli and Garcia (2000). The figure indicates that the overestimate in T_{11}^B variance in the tropical ocean regions seen in figure 4 occurs primarily at time scales of 2-10 days. Variance of longer and shorter time scales over oceans are much closer to observed values. Biases in variance are largest in the warm pool region of the equatorial pacific. Over oceans, both models and observations tend to place most of the variance at the 2-10 day timescales. There is a substantial difference between the spectral T42 and FV model configurations. There is not much difference between simulations including and excluding the slab ocean model. This implies our model clouds are not responding strongly to interactive surface temperature. All models tend to have too much variance at longer time scales (2-10 days), and not enough at shorter time scales (< 2 days).

Over land, the simulations look much closer to the observations. The basic partitioning of variance is much closer to the observations than over oceans across all frequency intervals. The FV model configuration shows somewhat more realistic features than the spectral model simulations there.

6 Precipitation Analysis

It is difficult to find reliable and robust estimates suitable for a climatological characterization of short timescale global precipitation events. There are vast expanses of the globe with limited availability of measurements, and the measurements in the more remote regions of the earth are frequently made as the opportunity occurs (e.g. ship track data). Dai (2001) analyzed 23 years of 3-hourly surface weather reports to document the diurnal cycle of precipitation occurrence for various types of precipitation over the globe. Dai and Trenberth (2004) used these surface observation to evaluate the CCSM2. That dataset allowed one to categorize the frequency of occurrence of precipitation type (drizzle, showery precipitation, snow, etc) but it did

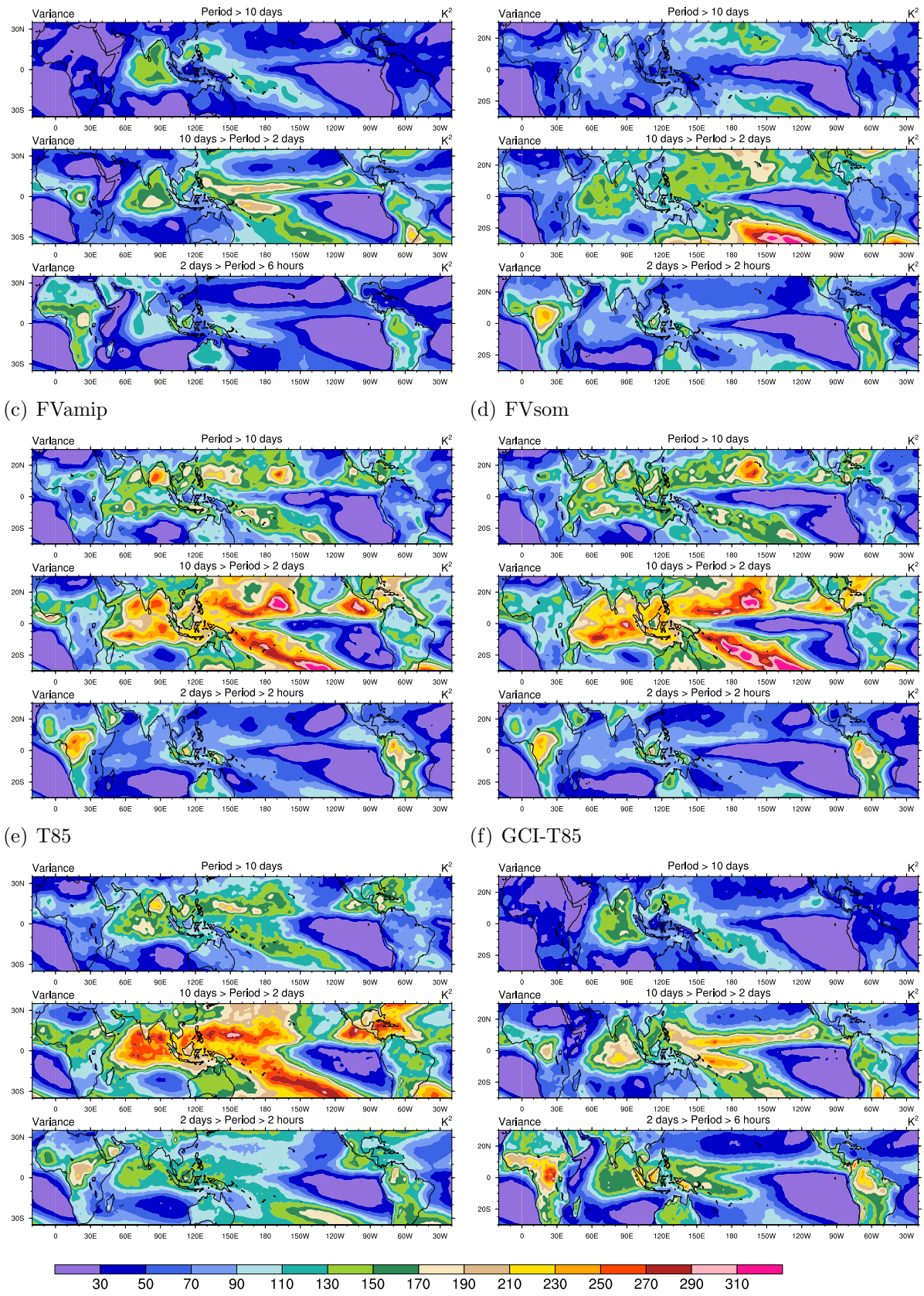

Figure 6: Annual average of the variance of T_{11}^B partitioned into frequency bins from the GCI dataset of Salby et al. (1991) and the CAM3 simulations.

not provide a quantitative measure of the intensity of the precipitation occuring in various regions of the world by hour of day.

Although TRMM measurements provide a good measure of precipitation locally, and globally over long time scales, it is of limited utility for sampling short time scale phenomena. The (TMI) produces only about 15 samples per year of the diurnal cycle at any locale. It revisits any given area at the same time infrequently (23 days at the equator and 46 days at midlatitudes). It thus provides limited information about short time scale variability, and is able to estimate features like the diurnal cycle of precipitation only by a compositing technique produced by examining the same location over a very long time for a region (Negri et al., 2002a). A fruitful method for estimating precipitation globally has been to use TRMM to calibrate another measured quantity which can produce high frequency retrievals of precipitation. One dataset that fits this description is the TRMM calibrated dataset 3B42. This is a product that first uses the TMI and VIRS IR measurements on TRMM to calibrate the algorithm, then applies the algorithm to merged geosynchronous data to produce a global three hour dataset. The 3B42 dataset includes only years 1998 and 1999.

Figure 7 shows the precipitation variance for three model runs in a format similar to figure 6. NB the contour intervals for the model runs (panel e) were chosen to be much smaller than the color bar for the precipitation retrievals (panel f), reflecting the fact that the current model configurations substantially underestimate variance in precipitation compared to the observational estimates. These figures may be compared to a similar set of figures in Ricciardulli and Garcia (2000) (their figures 2 and 4) who found that CCM3 underestimated the variance in precipitation at high frequencies, and in their case, overestimated the variance in the lower frequency band. The discrepancy between observational estimates and model simulations was substantially larger in RG00. They needed to change the contour interval by a factor of 10 between model and observational estimates to produce figures showing any signal. Our analysis suggests that CAM3 and the observations differ in variance by factors

of about 3 at the 2-10 day frequency interval and 4-5 in the higher frequency interval. As also seen in variance of T_{11}^B, discrepancies are largest over the tropical ocean. The observational estimate put most of the variance on the shortest time scales, while all model configuration to most of the variance in the 2-10 day time scale interval. Panels b-d do show that increasing the resolution increases the model variance at the 2-10 day timescales but decreases the variance at the shorter timescales. Over land, the discrepancies are much lower. The model puts most of the variance in the shorter time scale interval, and it is within 50% of the observational estimate.

Figure 8 shows composite diurnal cycles for 6 regions near the equator for JJA, at approximately the same latitude, but with quite different climatological regimes. The land regions (Africa and Tropical South America) are strongly influenced by heating and cooling of the land surface. The equatorial Indian ocean region is adjacent to and strongly influenced by the Indian monsoon. Oceanic ITCZ regions are located near the pacific warm pool, the cold pool, and the central Atlantic ocean respectively. We show estimates of the diurnal cycle for the T85 model, estimates following Negri et al. (2002b) from PR and TMI, and the IR calibrated 3B42 product. The ocean ITCZ regions all have a relatively weak diurnal variation. The Western Pacific ITCZ modelled and retrieved diurnal variation agree quite well. All show a mean value of 6-7 mm/day with an amplitude of diurnal variation of 2-3 mm/day. The peak precipitation occurs in the early morning hours. TMI and PR show maxima between midnight and 2AM LST. The IR product and CAM3 show a maximum about 3 hours later. The model and measurements agree less well over the other oceanic regions. The retrieved precipitation estimates in the Eastern pacific region tend to put the maximum value between 10-18 LST although the signal is very weak. The amplitude and time of maximum precipitation are consistent in the Atlantic ITCZ region between model and retrieval. All the model simulations estimate the maximum to occur in the morning hours. Agreement between model and retrievals is worst for the Indian Ocean region, where the model is almost out of phase with the observations.

(a) TRMM-3B42

(b) T42amip

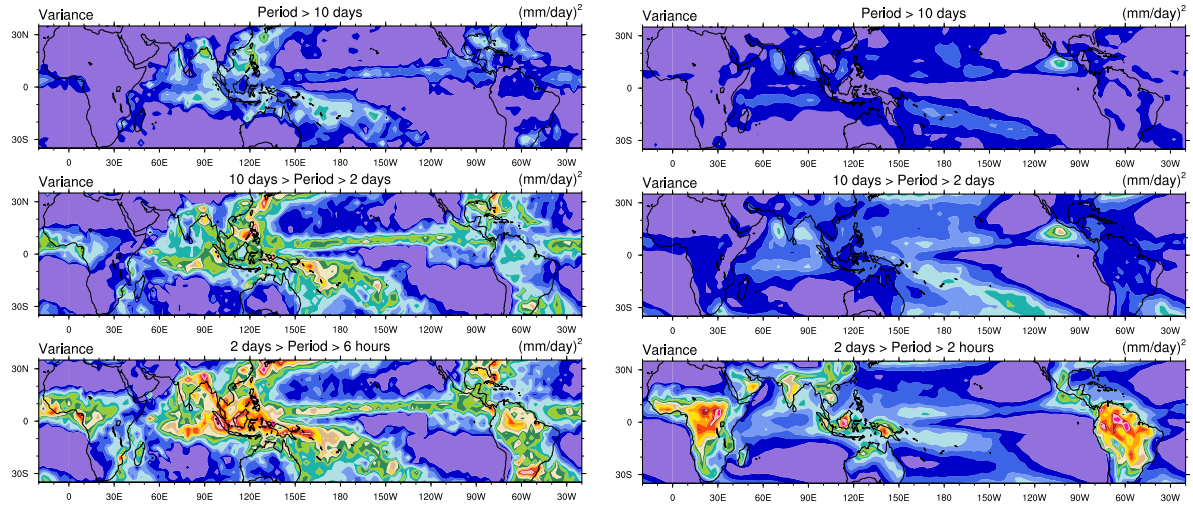

(c) FVamip

(d) T85amip

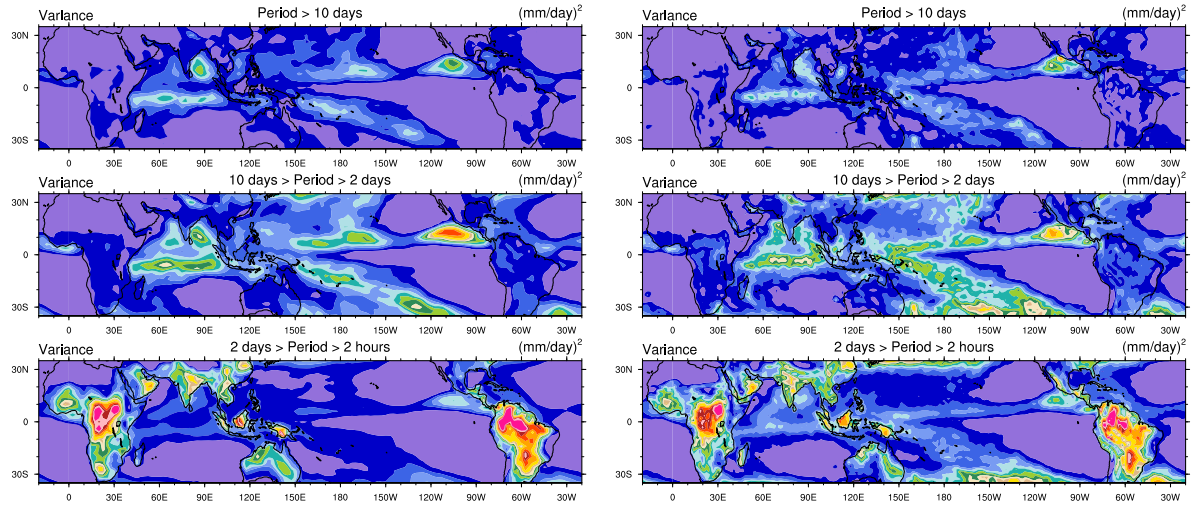

(e) Colorbar for panels b, c, and d:

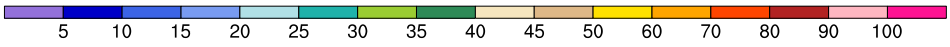

(f) Colorbar for panel a:

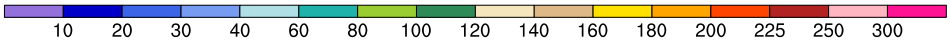

Figure 7: Annual average of the variance of precipitation partitioned into frequency bins from the TRMM 3B42 dataset (at T85 resolution, panel a) and the CAM3 simulations: (b) T42amip, (c) FVamip and (d) T85amip.

The continental regions show a much stronger diurnal variation. The observations show a semi-diurnal variation of precipitation with an early morning peak and a late afternoon peak. The model shows only the afternoon peak, and the amplitude of the diurnal variation tends to be stronger than that seen in the retrievals. The model tends to overestimate the diurnal cycle over land. The maximum occurs too early in the day over Africa, but not over northern South America. The model tends to underestimate nighttime precipitation in these regions. The 3B42 dataset again shows a few hour lag compared to the TMI or PR retrievals for these regions.

The spatial distribution of the amplitude and phase of the diurnal cycle of precipitation is shown in figure 9. Panels c and d show late afternoon precipitation over large tropical land masses, consistent in the 3B42-T85 and T85amip model run respectively. The models precipitation occurs 2-4 hours earlier than observations, but some caution is needed since it is well known that IR estimates of LST of precipitation maxima lag surface measurements (see Janowiak et al. (1994) and discussion surrounding figure 8). The amplitude of the diurnal cycle of precipitation over S. America is larger than observations. There is some evidence for topographic effects in vicinity of the Andes and Ethiopia, but it much weaker in the model than observations. The model clearly isn't resolving features that are known to be important in effecting land/sea and mountain valley breezes. The afternoon maximum in convection is over maritime land masses, surrounded by a morning maximum in convection off the coasts (Mapes and Houze, 1993), although again, only the larger islands of the maritime sub-continent are resolved by the model, even at T85 resolutions.

Over oceans the amplitude of the diurnal cycle is substantially underestimated, consistent with figure 7. The model amplitude is frequently between 0.2-0.3 of its mean value, while the observations suggest that it should be 0.3-0.5. The largest diurnal variation in relative terms occurs in regions where the precipitation is low, e.g. stratus and stratocumulus regions. The model diurnal variation produces a smaller contribution to the total in areas of intense precipitation (ITCZ and SPCZ)

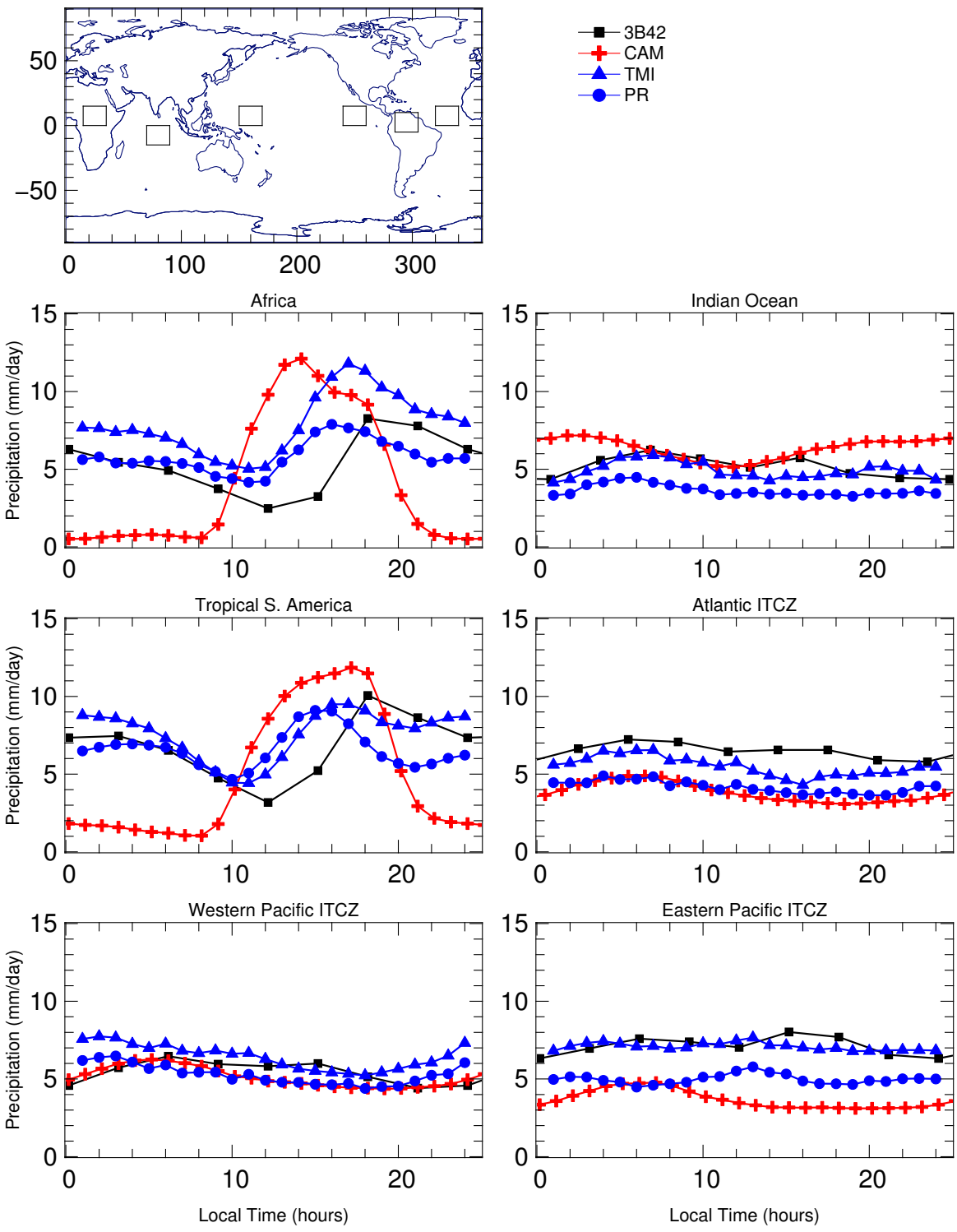

Figure 8: Regional composites of precipitation during JJA from the T85 version of the CAM3, and three observational estimates. TMI and PR estimates utilized 6 years of data (1998-2003). 3B42 dataset used data for 1998-1999. Five years of model simulation were used for the CAM3 estimate.

(a) 3B42

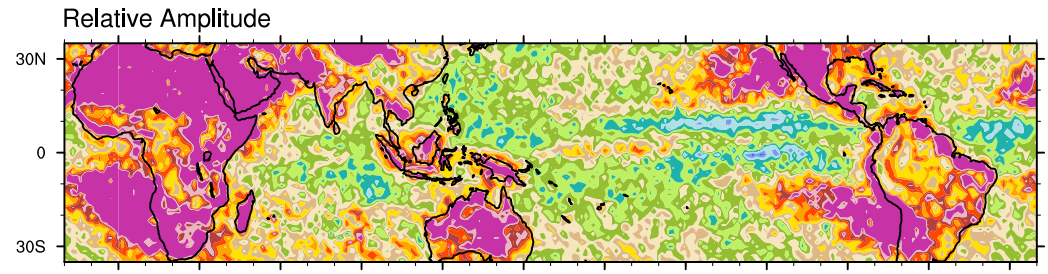

(b) T85amip

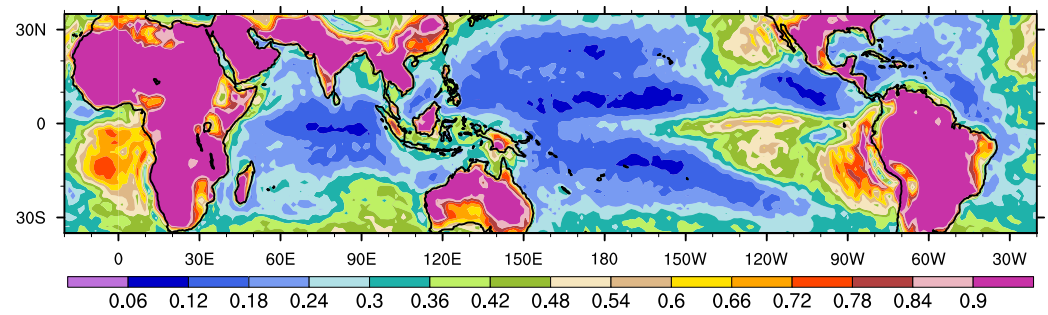

(c) 3B42

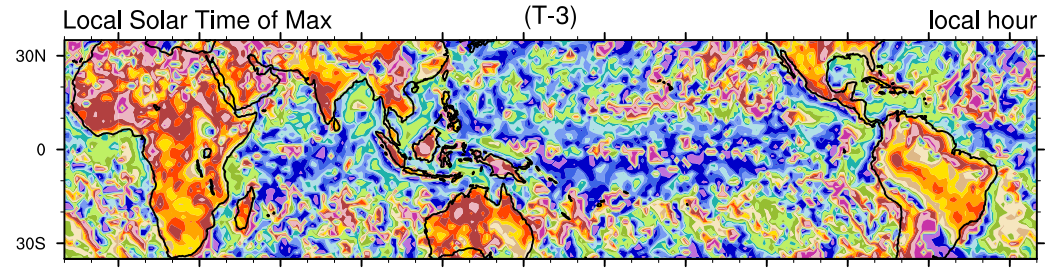

(d) T85amip

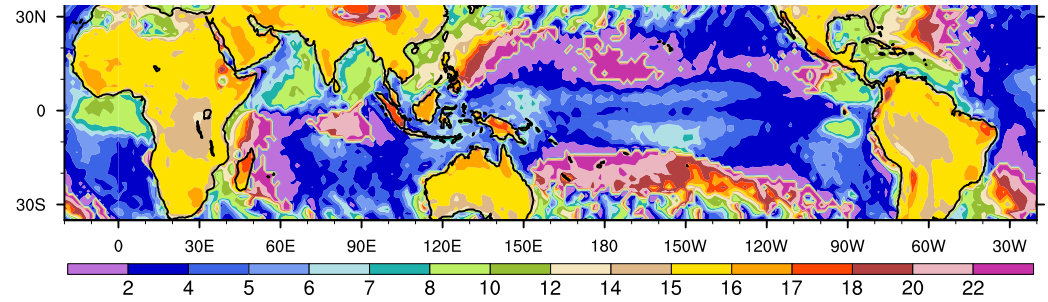

Figure 9: Comparison of diurnal cycle of the 3B42 precipitation Product and T85amip. The relative amplitude of the diurnal cycle appear in panels (a) and (b) respectively. Local Solar time of maximum precipitation the local time of precipitation max appears in (c) and (d). The LST of panel c has been shifted by 3 hours to account for the known lag of IR precipitation retrievals in estimating time of maximum precipitation.

and a higher contribution in subsidence regions (stratocumulus and trade cumulus regions). The same signal is seen the 3B42 dataset (panel a), but the difference between these regions of intense rain and other area of the globe are less pronounced than seen in the model.

To facilitate a comparison with the model, we have shifted the 3B42 estimate of time of maximum precipitation by three hours (earlier) to compensate for the known bias of the retrieved precipitation compared to raingauge or other surface measurements. Both observational estimates and the model frequently show the maximum in precipitation to occur between 2200 and 0600 over most of the tropical ocean. But the precipitation maxima occurs later much more frequently in the observational estimates than in the model. Both estimates show later times for precipitation in the Bay of Bengal, and near South America and the west coast of Africa (Gulf of Guinea). As seen in earlier version of CAM3 (Dai and Trenberth, 2004) the model tends to precipitate a few hour earlier over tropical land masses than seen in the observational estimate, with precipitation peaking between 1400-1600 LST in the model, and 1600-1800 LST in the observations.

Ricciardulli and Sardeshmukh (2002) have characterized the duration of precipitation events from observations and CCM3. We repeat one of their diagnostics using the 3B42 dataset and the T85amip, T42som, and FVsom versions of CAM3.

The upper panel shows the duration of precipitation events as gauged from the 3B42 dataset. Data with drizzle (rain $<$ 1 mm/day) has been filtered prior to the analysis to produce a clearer picture of the duration of substantial precipitation. The longest time scale events (8-10 hours) are seen in the ITCZ region of the Atlantic and Pacific oceans. Over other parts of the tropical oceans, the precipitation duration is 4-8 hours. The duration of events over tropical land masses, is also 4-8 hours or shorter.

The duration of precipitation for events for all model configurations (panels b, c, and d) is much longer. We have increased the colorbar scale by a factor of 4 to provide

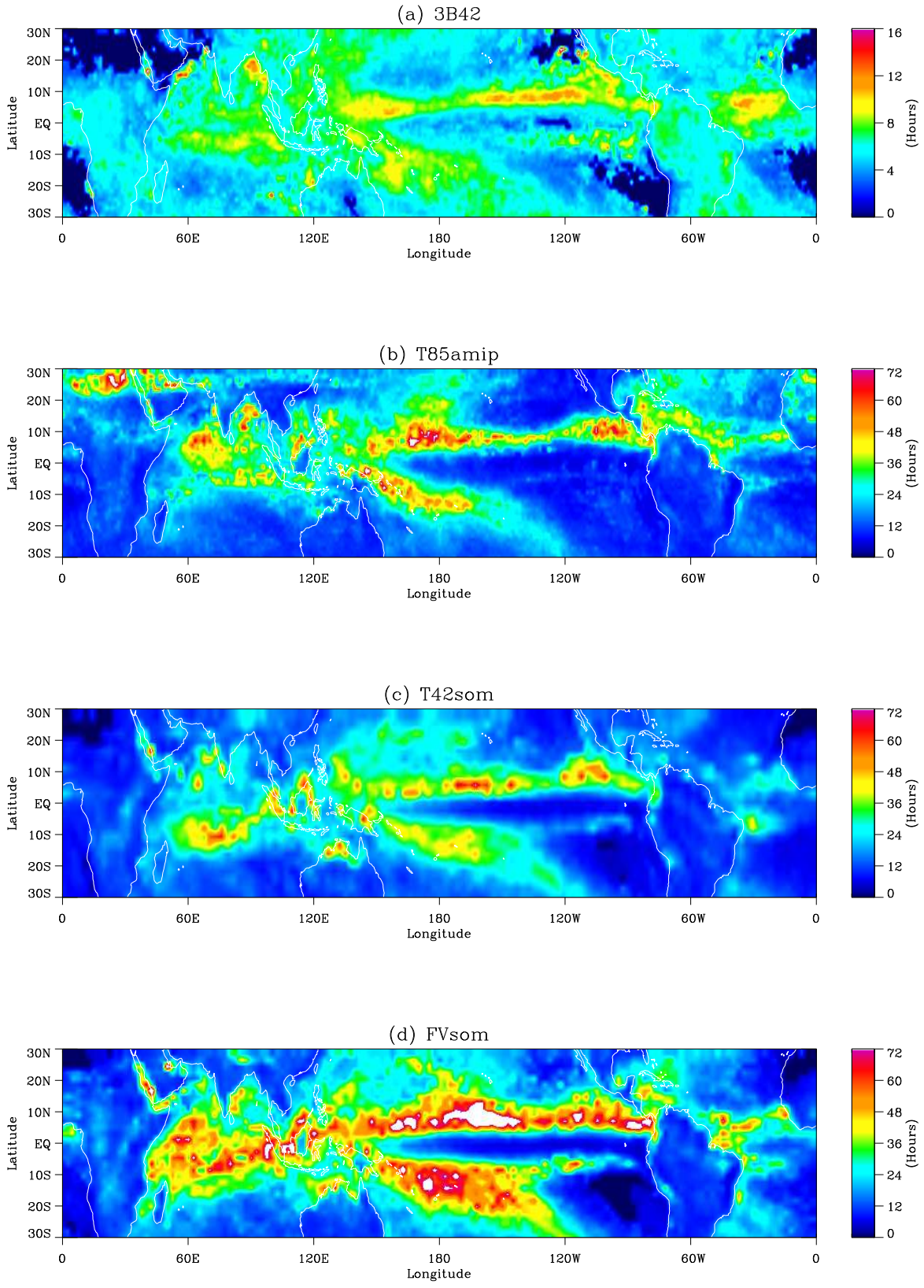

Figure 10: Duration of precipitation events derived from 3B42 and various model configurations. Note the change in scale for the observed and modelled precipitation duration.

information about the range of events seen in the model. Most oceanic precipitation events last as long as 36 hours, with the longest events persisting for up to 72 hours. Over land masses the precipitation events are as long as 12 hours.

7 Liquid water path.

Wood et al. (2002) have analyzed some aspects of the diurnal cycle of the liquid water path in the tropics and subtropics using TRMM TMI data with a focus on non-precipitating boundary layer clouds. The LWP retrieval for this dataset uses the algorithm from Wentz (1997). The retrieval is performed only over ocean surfaces for non precipitating clouds. Figure 11 shows the amplitude of the diurnal cycle, and estimated hour of maximum LWP from their analysis, compared to the T85amip version of CAM3 (where the hour is calculated for both precipitating and non-precipitating clouds). Both model and observations put the largest amplitude diurnal cycle in the southern hemisphere (off the west coast of south America and south Africa), in regions with large amounts of stratocumulus clouds. As noted by Wood et al. (2002), there is a strong asymmetry between northern and southern stratocumulus regions. The amplitude of the diurnal cycle is as much as a factor of two higher over much of the ocean regaion in the model compared to the TRMM retrieved value. It is not clear whether the exclusion of precipitating clouds in the TRMM retrieval can explain this difference. We have explored the consequences of excluding model cells in which there is no precipitation, but this dramatically reduces the liquid water path. Because the exclusion of precipitating clouds during the precipitation retrieval is done at a much finer spatial resolution, the impact may be much different than a procedure excluding the model columns at the lower resolution. Both model and observation indicate that the LST for maximum LWP occurs in the early morning (0-4) hours over most of the oceanic regions, although the model LWP maximum tends to occur an hour or two earlier than the observations. Both also show a maximum near local noon in the

Caribbean and the Bay of Bengal.

8 Summary and Conclusions

There are still many uncertainties in quantifying aspects of atmospheric transient associated with the hydrologic cycle. Space based retrievals are probably accurate only to 30% or so, and many of the best of those measurements are available for only a few years, which complicates the interpretation because of strong interannual variability. In spite of these uncertainties we believe that CAM still has a long way to go for a reasonable representation of tropical transient activity on less than 30 day time scales. Our results show that the transient aspects of convection are too weak, and that the connection between convection and stratiform clouds is underestimated.

The very strong connection observed between brightness temperature and precipitation in the observed atmosphere is much weaker in CAM3. The variance of brightness temperature on less than 30 day time scales has a strong sensitivity to resolution in CAM3. Lower resolution model run underestimate the observed variability. Higher resolution runs probably overestimate that variability, and the spatial extent of that variability, which tends to very strongly correlated with regions of strong convection over land and oceans. The transient variability is more sensitive to resolution than to the numerical method used to solve for the atmospheric dynamics and transport of water substances. The overestimate of variability in the model tends to occur at 2-10 day time scales. The shorter time scales (< 2 days) tend to be underestimated in the model.

Stratiform rain is shown to be about 10% of total rainfall in tropics, rather than the estimated 30-60% in the real atmosphere. Dai and Trenberth (2004) suggested that the underestimate of stratiform precipitation in CCSM2 was related to deficiencies in the moist convection scheme. They hypothesized that moist convection occured too frequently, and lasted too long, removing water vapor prematurely and too efficiently.

(a) TMI

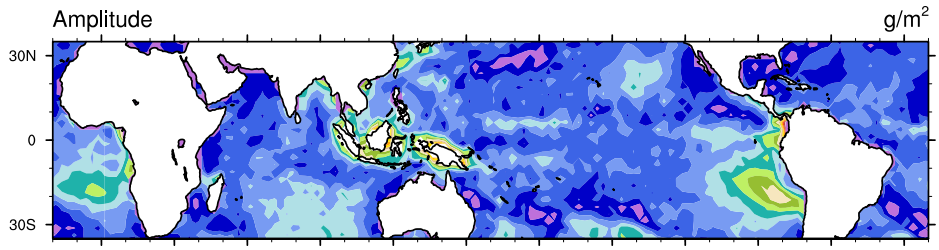

(b) T85amip

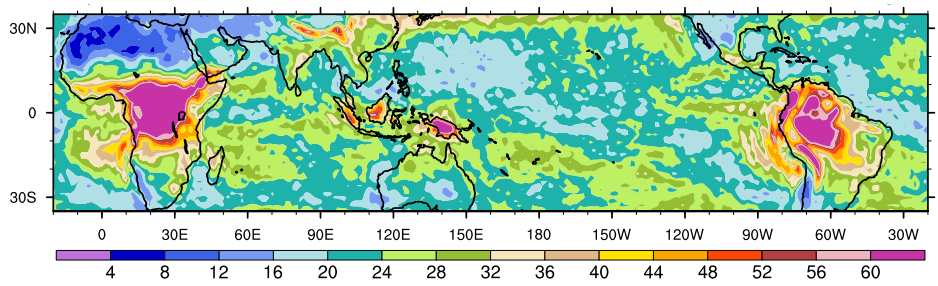

(c) TMI

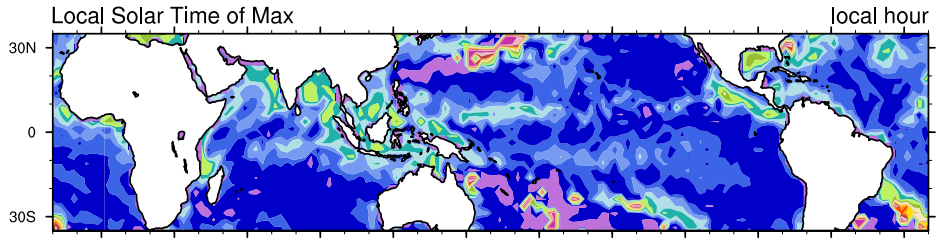

(d) T85amip

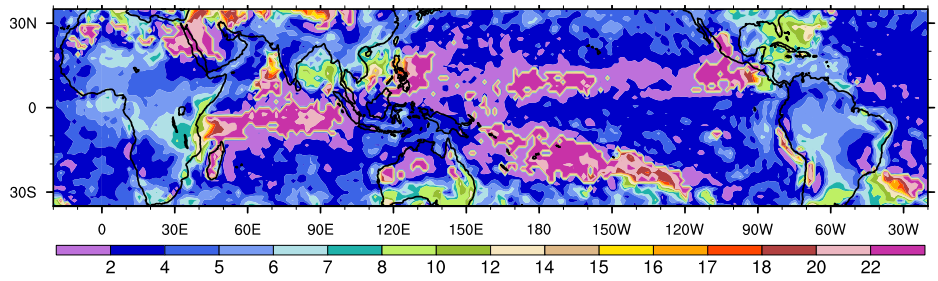

Figure 11: Amplitude of LWP diurnal cycle (panels a and b) and Local Solar time of maximum LWP (panels c and d) as estimated from the TRMM and the T85amip model configuration.

This conclusion is consistent with the study of Ricciardulli and Sardeshmukh (2002) and this study. We have shown that CAM3 precipitation events last much longer (as long as 60 hours) than those inferred from the space based retrievals at an equivalent resolution (about 12 hours).

Dai and Trenberth (2004) also showed that CCSM1 had too low diurnal variations of precipitation and cloud cover over oceans and speculated that it was due in part to the use of SSTs that included no diurnal variation. We have examined model runs that include surface properties that can evolve on sub-diurnal time scales, and there is little improvement in the model variability. This does not mean that diurnal varying SSTs are not important in influencing convection, but rather that some other necessary condition for diurnally varying convection may also be missing. Our results suggest that there must be some other explanation for the problems with diurnal variability. A likely candidate is the closure and tunable parameters in the convection scheme.

Most model configurations show similar behavior in terms of the transient variability. We found a strong sensitivity of modelled T_{11}^B to resolution. The sensitivity of the modelled rainfall variability to resolution was much smaller than that of T_{11}^B. All model configurations still underestimated the precipitation variability of the atmosphere over oceans. The underestimation is most severe at time scales shorter than two days, but the model variability is also too low on 2-10 day time scales. We estimate that the model is a factor of 3-5 too low in terms of the amplitude of the diurnal cycle of precipitation, which shows less discrepancy with observations than earlier versions of the model, but is still distressingly large. Increasing resolution does increase the variability in the precipitation fields, but it is not a viable solution to improving the lack of variance of the precipitation. Some other measure must be found. The maximum rainfall rate over oceans tends to occur in the early morning hours in both the model and the atmosphere, but (as in the studies with CAM3's predecessors the model peak comes a few hours earlier than the estimates for the atmosphere.

The diurnal variation over tropical land masses is represented more faithfully the over oceans in the model. The model still tends to overestimate the amplitude of the diurnal cycle, and it tends to rain too much during the day, and not enough at night.

Our results suggest that the model overestimates the diurnal variation of LWP, but because the retrieval of LWP was not done when precipitation is present the TRMM estimate may be underestimating the amplitude of the diurnal cycle by excluding clouds with the largest liquid water contents. (The TRMM TMI instrument retrieval uses information at about a 10km footprint to do the retrieval.) The largest diurnal variations in cloud LWP in model and observations are seen in the southern hemisphere off the west coast of the continents in regions typically occupied by stratocumulus clouds. Peak LWP occured later in the day in the Bay of Bengal and Caribbean. We did not attempt to identify the contributions to the LWP from variations of in-cloud water content versus cloud fraction.

It is clear that while there is a strong spatial correlation between T_{11}^B variance and precipitation variance in the model, there isn't a very strong correlation between brightness temperature and precipitation themselves in the model. The strong correlation between these fields in nature is the reason that IR retrieval techniques are so successful in producing accurate estimates of precipitation. This inconsistency in model behavior may serve as an indicator of "missing links" and what processes could be improved in the model.

In previous generations of the CAM most of our attention has been focussed on developing a model that provides reasonable fidelity to the atmosphere on seasonal, annual and interannual time scales. These features remain important, but it is clear that there are other meteorological features occuring at shorter time scales that we know to be important that are still poorly handled in the model. Our intention is to begin examining these features routinely in the ongoing effort to develop the next generation of CAM.

Acknowledgments We would like to thank Danielle Coleman, and Jim McCaa for assistance in model runs, and data analysis. We benefitted greatly from conversations with George Huffman and Tom Bell regarding TRMM data, PDFs, and general caveats about interpretation of satellite data.

References

Adler, R. F. and A. J. Negri, 1988: A satellite infrared technique to estimate tropical convective and stratiform rainfall. *J. Atmos. Ocean. Tech.*, **27**, 30–51.

Arkin, P. A. and B. N. Meisner, 1987: The relationship between large-scale convective rainfall and clod cloud over the wester hemisperire during 1982-1984. *Mon. Weather Rev.*, **115**, 51–74.

Bergman, J. W. and M. L. Salby, 1994: Equatorial wave activity dreived from fluctuation in observed convection. *J. Atmos. Sci.*, **51**, 3791–3806.

Bergman, J. W. and M. L. Salby, 1996: Diurnal variotions of cloud cover and their relationship to climatological conditions. *J. Climate*, **9**, 2802–2819.

Boville, B. A., P. J. Rasch and J. J. Hack, 2004: The impact of changing moist physical processes on the general circulation of CAM; Sensitivity studies. *J. Climate*, in preparation.

Bowman, K. P., A. B. Phillips and G. R. North, 2003: Comparison of TRMM rainfall retrievals with rain gauge data from the TAO/TRITON buoy array. *Geophys. Res. Lett.*, **30**, DOI 10.1029/2003GL017552.

Collier, J. C. and K. P. Bowman, 2004: Diurnal cycle of tropical precipitation in a general circulation model. *J. Geophys. Res.*, **109**, DOI 10.1029/2004JD004818.

Collins, W. D., P. J. Rasch, B. A. Boville, J. J. Hack, J. R. McCaa, D. L. Williamson, B. P. Briegleb, C. M. Bitz, S.-J. Lin, M. H. Zhang and Y. Dai, 2004a: The formulation and atmospheric simulation of the Community Atmosphere Model: CAM3. *J. Climate*, submitted.

Collins, W. D., P. J. Rasch, B. A. Boville, J. J. Hack, J. R. McCaa, D. L. Williamson, J. T. Kiehl, B. P. Briegleb, C. M. Bitz, S.-J. Lin, M. H.

643 Zhang and Y. Dai, 2004b: Description of the NCAR Community Atmo-
644 sphere Model: CAM3.0. Tech. Rep. NCAR/TN-464+STR, National Cen-
645 ter for Atmospheric Research, Boulder, Colorado, USA, 226 pp., URL =
646 `http://http://www.ccsm.ucar.edu/models/atm-cam`.

647 Dai, A., 2001: Global precipitation and thunderstorm frequencies. part II: Diurnal
648 variations. *J. Climate*, **14**, 1112–1128.

649 Dai, A. and K. E. Trenberth, 2004: The diurnal cycle and its depiction in the Com-
650 munity Climate System Model. *J. Climate*, **17**, 930–951.

651 Denning, A. S., D. Randall, G. Collatz and P. Sellers, 1996: Simulations of terrestrial
652 carbon metabolism and atmospheric CO2 in a general circulation model. part 2:
653 Spatial and temporal variations of atmospheric CO2. *Tellus*, **48B**, 543–567.

654 Hack, J. J., 2004: Impacts of horizontal resolution. *J. Climate*, submitted.

655 Hack, J. J., J. M. Caron, S. G. Yeager, K. W. Oleson, M. M. Holland, J. E. Truesdale
656 and P. J. Rasch, 2004: The simulation of the global hydrological cycle in the CCSM
657 community atmosphere model CAM3: Mean state. *J. Climate*, submitted.

658 Hartmann, D. L., H. H. Hendon and J. R. A. Houze, 1984: Some implications of
659 the mesoscale circulations in tropical cloud clusters for large-scale dynamics and
660 climate. *J. Atmos. Sci.*, **41**, 113–121.

661 Hendon, H. H. and K. Woodberry, 1993: The diurnal cycle of tropical convection. *J.*
662 *Geophys. Res.*, **98**, 16623–16637.

663 Houze, R. A., 1997: Stratiform precipitation in regions of convection: A meteorolog-
664 ical paradox? *Bull. Am. Meteorol. Soc.*, **78**, 2179–2196.

665 Houze, R. A., C. CHeng, C. A. Leary and J. F. Gamache, 1980: Diagnosis of cloud
666 mass and heat fluxes from radar and synoptic data. *J. Atmos. Sci.*, **37**, 754–773.

667 Huffman, G. J., R. F. Adler, P. Arkin, A. Chang, R. Ferraro, A. Gruber, J. Janowiak,
668 A. McNab, B. Rudolf and U. Schneider, 1997: The global precipitation climatology
669 project (GPCP) combined precipitation dataset. *Bull. Am. Meteorol. Soc.*, pp. 5–
670 20.

671 Janowiak, J., P. A. Arkin and M. Morrissey, 1994: An examination of the diurnal
672 cycle in oceanic tropical rainfall using satellite and in situ data. *Mon. Weather*
673 *Rev.*, **122**, 2296–2311.

674 Jorgensen, D. P. and M. A. LeMone, 1989: Vertical velocity characteristic of oceanic
675 convection. *J. Atmos. Sci.*, **46**, 621–640.

676 Kiehl, J. T., W. D. Collins, J. J. Hack and C. Shields, 2004: The climate sensitivity
677 of CCSM3. *J. Climate*, submitted.

678 Kummerow, C., R. Kakar, F. Wentz, P. Ashcroft, T. Kozu, Y. Hong, K. O. T. Iguchi,
679 H. Kuroiwa, E. Im, Z. Haddad, G. Huffman, B. Ferrier, W. S. Olson, E. Zipser,
680 E. A. Smith, T. T. Wilheit, G. North, T. Krishnamurti and K. Nakamura, 2000:
681 The status of the Tropical Rainfall Measuring Mission (TRMM) after two years in
682 orbit. *J. Appl. Meteorol.*, **39**, 1965–1982.

683 LeMone, M. A. and E. J. Zipser, 1980: Cumulonimbus vertical velocity events in
684 GATE. part I: diameter, intensity and mass flux. *J. Atmos. Sci.*, **37**, 2444—2457.

685 Mapes, B. E. and R. A. Houze, 1993: Cloud clusters and superclusters over the
686 oceanic warm pool. *Mon. Weather Rev.*, **121**, 1398–1415.

687 Masunaga, H., T. Iguchi, R. Oki and M. Kachi, 2002: Compareison of rasinfall prod-
688 ucts derived from TRMM microwave imager and precipitation radar. *J. Appl. Me-*
689 *teorol.*, **41**, 849–862.

690 Meisner, B. N. and P. A. Arkin, 1987: Spatial and annual variations in the diurnal

691 cycle of large scale tropical convective cloudiness and preciptation. *Mon. Weather*
692 *Rev.*, **115**, 2009–2031.

693 Minnis, P., D. F. Young and E. F. Harrison, 1991: Examination of the relationship
694 between outgoing infrared window and total longwave fluxes using satellite date.
695 *J. Climate*, **4**, 1114–1133.

696 Negri, A. J., R. F. Adler and L. Xu, 2002a: A TRMM-calibrated infrared rainfall algo-
697 rithm applied over Brazil. *J. Geophys. Res.*, **107**(D20), doi:10.1029/2000JD000265.

698 Negri, A. J., T. Bell and L. Xu, 2002b: Sampling of the diurnal cycle of precipitation
699 using TRMM. *J. Atmos. Ocean. Tech.*, **19**, 1333–1344.

700 Ohring, G., A. Gruber and R. Ellingson, 1984: Satellite determinations of the rela-
701 tionship between total longwave radiation flux and infrared window radiance. *J.*
702 *Clim. Appl. Meteorol.*, **23**, 416–425.

703 Rasch, P. J., 2004: Characteristics of transport using three formulations of atmo-
704 spheric dynamics in a single GCM framework. *J. Climate*, in preparation.

705 Ricciardulli, L. and R. Garcia, 2000: The excitation of equatorial waves by deep
706 convection in the NCAR Community Climate Model. *J. Atmos. Sci.*, **57**, 3461–
707 3487.

708 Ricciardulli, L. and P. D. Sardeshmukh, 2002: Local time- and space scales of orga-
709 nized tropical deep convection. *J. Climate*, **15**, 2775–2789.

710 Richards, F. and A. Arkin, 1981: On the relationship between satellit observed cloud
711 cover and precipitation. *Mon. Weather Rev.*, **109**, 1081–1093.

712 Salby, M. L., H. H. Hendon, K. Woodberry and K. Tanaka, 1991: Analysis of global
713 cloud imagery from multiple satellites. *Bull. Am. Meteorol. Soc.*, **72**, 467–480.

714 Schumacher, C. and R. A. Houze, 2003: Stratiform rain the trhe tropics as seen by
715 the TRMM precipitation radar. *J. Climate*, **16**, 1739–1756.

716 Scinocca, J. F. and N. McFarlane, 2004: The variability of modeled tropical precipi-
717 tation. *J. Atmos. Sci.*, **61**, 1993–2015.

718 Song, X. and R. Yu, 2004: Underestimated tropical stratiform precipitation in the
719 National Center for Atmospheric Research (NCAR) Community Climate Model
720 (CCM3). *Geophys. Res. Lett.*, **31**, DOI: 10.1029/2004GL021292.

721 Takahashi, M., 1999: Simulation of the quasi-biennial oscillation in a general circula-
722 tion model. *Geophys. Res. Lett.*, **26**, 1307–1310.

723 Wentz, F. J., 1997: A well-calibrated ocean algorithm for special sensor mi-
724 crowave/imager. *J. Geophys. Res.*, **102**, 8703–8718.

725 Wood, R., C. S. Bretherton and D. L. Hartmann, 2002: Diurnal cycle of liquid
726 water path over the subtropical and tropical ocean. *Geophys. Res. Lett.*, **26**(23),
727 DOI:10.1029/2002GL015371.

728 Yang, G.-Y. and J. Slingo, 2001: The diurnal cycle in the tropics. *Mon. Weather*
729 *Rev.*, **129**, 784–801.